

# Cloth-Changing Person Re-identification from A Single Image with Gait Prediction and Regularization

Xin Jin<sup>1\*</sup> Tianyu He<sup>2\*</sup> Kecheng Zheng<sup>1</sup> Zhiheng Yin<sup>3</sup> Xu Shen<sup>2</sup> Zhen Huang<sup>1</sup>  
 Ruoyu Feng<sup>1</sup> Jianqiang Huang<sup>2</sup> Zhibo Chen<sup>1†</sup> Xian-Sheng Hua<sup>2†</sup>

<sup>1</sup> University of Science and Technology of China <sup>2</sup> DAMO Academy, Alibaba Group <sup>3</sup> University of Michigan

jinxustc@mail.ustc.edu.cn

## Abstract

Cloth-Changing person re-identification (CC-ReID) aims at matching the same person across different locations over a long-duration, e.g., over days, and therefore inevitably meets challenge of changing clothing. In this paper, we focus on handling well the CC-ReID problem under a more challenging setting, i.e., just from a single image, which enables high-efficiency and latency-free pedestrian identify for real-time surveillance applications. Specifically, we introduce **Gait** recognition as an auxiliary task to drive the **Image ReID** model to learn cloth-agnostic representations by leveraging personal unique and cloth-independent gait information, we name this framework as **GI-ReID**. **GI-ReID** adopts a two-stream architecture that consists of a image ReID-Stream and an auxiliary gait recognition stream (Gait-Stream). The Gait-Stream, that is discarded in the inference for high computational efficiency, acts as a regulator to encourage the ReID-Stream to capture cloth-invariant biometric motion features during the training. To get temporal continuous motion cues from a single image, we design a Gait Sequence Prediction (GSP) module for Gait-Stream to enrich gait information. Finally, a high-level semantics consistency over two streams is enforced for effective knowledge regularization. Experiments on multiple image-based Cloth-Changing ReID benchmarks, e.g., LTCC, PRCC, Real28, and VC-Clothes, demonstrate that **GI-ReID** performs favorably against the state-of-the-arts. Codes are available at <https://github.com/jinx-USTC/GI-ReID>

## 1. Introduction

Person re-identification (ReID) aims at identifying a specific person across cameras, times, and locations. Abundant approaches have been proposed to address the challenging geometric misalignment among person images caused



Figure 1: (a) shows a realistic wanted case that a suspect changed her coat from black to white for hiding. (b) reveals that the gait of person could help ReID, especially when the identity matching meets the cloth-changing challenge (All faces in the images are masked for anonymization).

by diversities of human poses [52, 72, 46], camera view-points [68, 54, 23], and style/scales [25, 24]. These methods usually inadvertently assume that both query and gallery images of the same person have the *same clothing*. In general, they perform well on the trained short-term datasets but suffer from significant performance degradations when testing on a long-term collected ReID dataset [63, 48, 65, 57]. Because large clothing variations occur over long-duration among these datasets, which seriously hinders the accuracy of ReID. For example, Figure 1(a) shows a realistic wanted case<sup>1</sup> where a suspect that captured by surveillance devices at different times/locations changed her coat from black to white, which makes ReID difficult, especially when she wears a mask and the captured images are of low quality.

In recent years, to handle the cloth-changing ReID (CC-ReID) problem, some studies have contributed some new datasets where clothing changes are commonplace (e.g., Celebrities-reID [20, 19], PRCC [63], LTCC [48], Real28 and VC-Clothes [57]). They also propose some new al-

\*The first two authors contribute equally to this work.

†Corresponding Author.

<sup>1</sup>Information comes from <https://www.wjr.com/2016/01/06/woman-wanted-in-southwest-detroit-bank-robbery/>

gorithms that could learn cloth-agnostic representations for CC-ReID. For instance, Yang *et al.* [63] propose a contour-sketch-based network to overcome the moderate cloth-changing problem. Similarly, Qian *et al.* [48] and Li *et al.* [34] both explore to utilize body shape information to tackle the CC-ReID problem. However, no matter of using contour sketch or body shape, these methods are all prone to suffer from estimation error problem. Because single-view contour/shape inference (from 2D image) is extremely difficult due to the vast range of possible situations, especially when people wear thick clothes in winter. Besides, these contour-sketch-based or shape-based methods only focus on extracting *static spatial cues* from persons as extra cloth-invariant representations, the rich *dynamic motion information* (e.g., gait) of human that can be predicted (i.e., implied motion [30]) even from a single 2D image are often ignored.

Another popular branch for CC-ReID is to extract face/hairstyle features as cloth-invariant characteristics [62, 65, 57]. However, this kind of methods tend to fail for at least two reasons. First, biometric traits like face/hairstyle is too weak to be learned, because they only take up a small part of the body image. Besides, the model hardly learn discriminative human representations if we only utilize unclear/masked face information.

In this paper, we explore to leverage the unique gait features that imply dynamic motion cues of pedestrian to drive a model to learn cloth-agnostic and discriminative ReID representations. As shown in Figure 1(b), although it is hard to identify the same person when he/she wears different clothes, or to distinguish the different persons when they wear similar/same clothes, we can still leverage their unique/discriminative gaits to achieve correct identity matching. It is because that gait, as an unique biometric feature, has superior invariance compared with other easy-changing appearance characteristics (e.g., face, body shape, contour). Besides, gait can also be authenticated at a long distance even with low-quality camera imaging.

Unfortunately, existing gait-related studies mainly rely on large video sequences [3, 9]. Capturing videos requires time latency and saving videos needs a large hardware storage cost, which are both undesirable for real-time surveillance ReID applications. How to leverage gait feature to handle CC-ReID problem just using a single image, has not been deeply studied and is more challenging/practical.

Therefore, we propose a **Gait-assisted Image-based ReID** framework, termed as GI-ReID, which could learn cloth-agnostic ReID representations from a single image with the gait feature assistance. GI-ReID consists of a main image-based ReID-Stream and an auxiliary gait recognition stream (Gait-Stream). Figure 2 shows the entire framework. The Gait-Stream aims to regularize the ReID-Stream to learn cloth-agnostic features from a single RGB image for effective CC-ReID. It is discarded in the inference for the

high efficiency. Since the comprehensive gait features extraction typically needs a gait video sequence as input [3, 9], we design a new Gait Sequence Prediction (GSP) module for Gait-Stream to approximately forecast continuous gait frames from a single input query image, which makes our GI-ReID framework more general. Finally, to encourage the main ReID-Stream’s efficient learning from Gait-Stream, we further enforce a high-level Semantics Consistency (SC) constraint for the same person over two streams’ features. We summarize our main contributions as follows:

- We specially aimed at handling the challenging cloth-changing issue for image ReID, which further bridges the gap between ReID algorithms and practical applications.
- A Gait-assisted Image-based cloth-changing ReID (GI-ReID) framework is proposed. The Gait-Stream in GI-ReID, as a regulator, can be removed in the inference without affecting ReID results. This reduces the dependency on the performance of the gait recognition, making our method more computationally efficient and robust.
- A well-designed Gait Sequence Prediction (GSP) module makes our method effective in the challenging image-based ReID scenarios. And, a high-level semantics consistency constraints enables an effective regularization over two streams, enhancing the distinguishing power of ReID-Stream under cloth-changing setting.

With the prediction and regularization of gait features, our GI-ReID achieves state-of-the-art performance when meets changing clothes, especially on the image ReID scenarios. GI-ReID framework is also general enough to be compatible with existing ReID-specific backbone networks.

## 2. Related Work

### 2.1. Person Re-identification

**General ReID.** General ReID, i.e., without cloth-changing cases, has achieved great success with the development of deep learning. It includes exploring part-level/fine-grained pedestrian feature descriptions [55, 58, 10, 76], and addressing the challenge of spatial misalignment caused by (a) different camera viewpoints [53, 23], (b) different poses [52, 11, 46], (c) semantics inconsistency [71, 25], (d) occlusion/partial-observation [77, 41, 75, 15], *etc.*

The above methods rely substantially on static texture information. However, when person ReID meets changing clothes, the texture information is not so reliable since it changes significantly even for the same person. Compared to static texture, the gait information, as a discriminative biometric modality, is more consistent and reliable under the clothing change scenarios.

**Cloth-Changing ReID.** Considering the wider application range and greater practical value of Cloth-Changing ReID (CC-ReID), more and more studies pay their attention to solving this challenging problem. Huang *et al.* [20, 19] pro-



### 3. Proposed GI-ReID Framework

GI-ReID framework aims to fully exploit the unique human gait information to handle the cloth-changing challenge of ReID just depending on a single image. Figure 2 shows the flowchart of the entire framework. Given a single person image, its mask/silhouette will be first extracted as input to the Gait-Stream using SOTA semantic segmentation methods, such as PointRend [27]. With the proposed gait sequence prediction (GSP) module, we could predict a gait sequence with more comprehensive gait information, which is then fed into the subsequent recognition network (GaitSet [3]) to extract discriminative gait features. Through a high-level semantics consistency (SC) constraint, the cloth-independent Gait-Stream acts as a regulator to encourage the main ReID-Stream to capture cloth-agnostic features from a single RGB image. We discuss the details of each component in the following sections.

#### 3.1. The Auxiliary Gait-Stream

Gait-Stream is composed of two parts: Gait Sequence Prediction (GSP) module and the pre-trained gait recognition network (GaitSet [3]). GSP is designed for gait information augmentation and GaitSet then extracts cloth-independent and discriminative motion feature cues from augmented gait to guide/regularize ReID-Stream’s training.

**Gait Sequence Prediction (GSP) Module:** GSP module aims to predict a gait sequence that contains continuous gait frames. This module is related to the general video frame prediction task (*i.e.*, frame interpolation and extrapolation studies [44, 18, 37, 13]), and gait sequence prediction can be deemed as a ‘gait frame synthesis’ process.

As shown in Figure 2, GSP is based on an auto-encoder architecture [7] with feature encoder  $E$  and decoder  $D$ . In order to reduce the prediction ambiguity and difficulty (*e.g.*, given a dangling arm, it is hard to guess whether it will rise or fall in the next second), we manually integrate the extra prior information of **middle frame index** into the inner learned feature through a position embedder  $P$  and a feature aggregator  $A$ . Intuitively, the **middle frame index** means that the input gait frame corresponds to the middle one of the predicted gait sequence, such prior knowledge will drive GSP module to predict the adjacent walking statuses *before* and *after* the current input walking status.

(1). **Encoder.** Given a silhouette input  $S$ , the encoder  $E$  aims to extract a dimension-shrunk compact feature:

$$f_S = E(S), \quad (1)$$

specific/detailed network structures (including other components in Gait-Stream) can be found in **Supplementary**.

(2). **Position Embedder and Feature Aggregator.** Considering the prediction ambiguity [40], we introduce a *middle frame input principle*, which ensures that the input sil-

houette correspond to the **middle** one of the gait frame sequence to be predicted. During the GSP training, we take the gait frame in the middle position of the ground truth gait sequence as input to GSP, and use a one-dimensional vector  $p \in \mathbb{R}^1$ , to denote such *position label*. Given a ground truth gait sequence with  $N$  frames, the position label  $p_{mid} \in \mathbb{R}^1$  of the input middle gait is defined as  $p_{mid} = N/2$  which indicates the relative position relationship of input gait frame to the entire sequence. For convenience, we convert position label to one-hot vector to calculate loss during the training. In formula, the position embedder  $P$  works as follows,

$$\tilde{p} = P(S) \in \mathbb{R}^1, \quad \mathcal{L}_{position} = \|\tilde{p} - p_{mid}\|_2^2, \quad (2)$$

where we compare the embedded position output  $\tilde{p}$  with the ground truth  $p_{mid}$  to construct a *position loss* as  $\mathcal{L}_{position}$ .

Feature aggregator  $A$ , implemented by a fully connected layer, is inserted between the encoder and the decoder to convert the raw encoded features  $f_S$  into *middle-position-aware* features  $f_S^{\tilde{p}}$  by taking the embedded middle position information  $\tilde{p}$  into account for the following decoder, which explicitly tells the decoder that we need to predict the gait statuses *before* and *after* the current input middle gait status, and thus reduces prediction variations in the predicted results. This feature aggregation process is formulated as,

$$f_S^{\tilde{p}} = A([f_S, \tilde{p}]), \quad (3)$$

where  $[\cdot]$  means a simple concatenation.

(3). **Decoder.** We feed the aggregated feature  $f_S^{\tilde{p}}$  into the decoder  $D$ , which has a symmetrical structure to that of the encoder  $E$ , to predict the gait sequence with a pre-defined fixed number of frames  $N$ . Such process is formulated as,

$$\tilde{R} = D(f_S^{\tilde{p}}) \in \mathbb{R}^{N \times h \times w}, \quad \mathcal{L}_{pred.} = \|\tilde{R} - GT\|_2^2, \quad (4)$$

where  $(h, w)$  denotes the (*height, width*) of predicted gait frames, same as the input silhouette image. A prediction loss  $\mathcal{L}_{pred.}$  is calculated to ensure the predicted gait sequence results is consistent with the ground truth (GT).

**Gait Feature Extraction:** The predicted gait sequence  $\tilde{R}$  is fed into pre-trained GaitSet [3] to learn discriminative and cloth-independent gait feature  $g$ . GaitSet is a set-based gait recognition model that takes a set of silhouettes as an input and aggregates features over frames into a set-level feature, which is formulated as  $g = \text{GaitSet}(\tilde{R})$ . More details are presented in **Supplementary**.

#### 3.2. The Main ReID-Stream

The backbone of the ReID-Stream could be any of the off-the-shelf networks, such as commonly-used ResNet-50 [14], ReID-specific PCB [55], MGN [58], and OS-Net [76]. And, we use the widely-adopted classification loss [55, 10], and triplet loss with batch hard mining [16]) on the ReID feature vector  $r$  as basic optimization objectives for training. The feature  $r$  is finally used for reference.



### 3.3. Joint Learning of Two Streams

Due to the potential rough mask/silhouette extraction and gait sequence prediction errors of GSP module, it is very difficult to directly exploit the gait information alone to complete effective ReID. Experimentally, we have attempted to conduct CC-ReID with only the predicted gait sequence  $\tilde{R}$  as input, and found this scheme failed to deliver good results (see ablation study for more details). Therefore, to exploit the cloth-independent merits of the gait information while avoiding the above-mentioned issues, we propose to jointly train Gait-Stream and ReID-Stream through a high-level semantics consistency (SC) constraint, where gait characteristics is taken as a regulator to drive the ReID-Stream’s cloth-agnostic feature learning. Note that the SC constraints are also not needed in the inference.

**Semantics Consistency (SC) Constraints.** SC constraints are essentially related to the common feature learning works, such as knowledge distillation [17], mutual learning [70], and knowledge amalgamation [64]. Our SC constraints differs from them mainly in two perspectives: 1) SC is to encourage high-level common feature learning from two modalities (dynamic gait and static RGB image). 2) SC ensures information integrity for each stream/modality.

The details of the SC constraints are shown in Figure 2. The learned gait feature  $g$  of Gait-Stream and ReID feature  $r$  of ReID-Stream are first transformed to a common and interactable space, via an embedding layer:  $\hat{r} = \text{Embed}(r)$  and  $\hat{g} = \text{Embed}(g)$ , where  $\hat{r}$  and  $\hat{g}$  have the same feature dimensions. Then, we enforce the transformed features  $\hat{r}$  and  $\hat{g}$  to be closed to each other by minimizing the Maximum Mean Discrepancy (MMD) [12]. MMD is a distance metric to measure the domain mismatch for probability distributions. We use it to measure the high-level semantics discrepancy between the transformed features  $\hat{r}$  and  $\hat{g}$ , and minimize it to drive ReID-Stream to pay more attention to cloth-independent gait biometric. An empirical approximation to the MMD distance of  $\hat{r}$  and  $\hat{g}$  is computed as follows:

$$\mathcal{L}_{MMD} = \|\mu(\hat{g}) - \mu(\hat{r})\|_2^2 + \|\sigma(\hat{g}) - \sigma(\hat{r})\|_2^2, \quad (5)$$

where  $\mu(\cdot), \sigma(\cdot)$  denotes the calculation of mean, variance of the distributions of transformed features  $\hat{r}$  and  $\hat{g}$ .

To avoid the information lost caused by feature regularization with SC constraints, we further enforce a reconstruction penalty to ensure that the transformed features  $\hat{g}$  and  $\hat{r}$  could be recovered to original versions. Specifically, we reconstruct the original output feature through a *Recon.* layer (implemented by FC layer):  $\tilde{r} = \text{Recon.}(\hat{r})$  and  $\tilde{g} = \text{Recon.}(\hat{g})$ , and calculate the corresponding reconstruction loss as follows:

$$\mathcal{L}_{recon.} = \|\tilde{g} - g\|_2^2 + \|\tilde{r} - r\|_2^2. \quad (6)$$

**Joint Training.** When we jointly training Gait-Stream and ReID-Stream on the ReID datasets, Gait-Stream is also fine-

tuned/learnable. Since the gait sequence ground truth are not available for ReID datasets, we adjust the original prediction loss  $\mathcal{L}_{pred.}$  in GSP by only calculating L1 distance between the single input gait mask and the *middle frame result* of the entire predicted gait sequence. More details of training process are provided in **Supplementary**, including pseudo code and loss balance strategy.

## 4. Experiment

### 4.1. Datasets, Metric and Experimental Setups

**Dataset Details.** We use one general video ReID dataset MARS [73] (to highlight the difficulty and necessity of image-based CC-ReID), and four recent cloth-changing ReID datasets Real28 [57], VC-Clothes [57], LTCC [48], PRCC [63] to perform experiments. Table 8 gives a brief information and comparison of these ReID datasets. More detailed introductions can be found in **Supplementary**.

Table 1: Brief introduction/comparison of datasets.

	MARS	Real28	VC-Clothes	LTCC	PRCC
Category	Video	Image	Image	Image	Image
Photo Style	Real	Real	Synthetic	Real	Real
Scale	Large	Small	Large	Large	Large
Cloth Change	No	Yes	Yes	Yes	Yes
Identities	1,261	28	512	152	221
Samples	20,715	4,324	19,060	17,138	33,698
Cameras	6	4	4	N/A	3
Usage	Train&Test	Test	Train&Test	Train&Test	Train&Test

**Evaluation Metrics.** We use the cumulative matching characteristics (CMC) at Rank-1/-10/-20, and mean average precision (mAP) to evaluate the performance.

**Experimental Setups.** We build **three** kinds of different experiment settings to comprehensively validate the effectiveness of gait biometric for cloth-changing ReID, and also validate the rationality/superiority of the proposed gait prediction and regularization in our GI-ReID framework:

**1) General Video ReID.** In this setting, we use a general video ReID dataset MARS for experiments. This dataset has no cloth-changing cases. This group of experiments aims to verify two things: 1) gait could benefit ReID even without clothes variations. 2) extracting gait feature from video is easier than that from image, or said, exploiting gait feature in the image-based CC-ReID is more challenging. Since MARS itself contains continuous video frames/clips and human gait masks<sup>2</sup>, we don’t need GSP to additionally predict gait sequence, so we discard it for simplicity.

**2) Imitated Cloth-Changing Video ReID.** We still use MARS as dataset to perform experiments in this setting. But the difference is that we *imitate* cloth-changing cases for the images with the same identity through a data augmentation strategy—body-wise color jitter (*i.e.*, randomly

<sup>2</sup>Human masks come from [https://pan.baidu.com/s/16ZrIM1f.1\\_T-eZHmQTTkYg](https://pan.baidu.com/s/16ZrIM1f.1_T-eZHmQTTkYg). We compare using mask for ReID, see **Supplementary**.

change the brightness, contrast and saturation of the human body region in an person image) for training. This group of experiments aims to show that gait information could alleviate the ReID interference caused by clothes changing. GSP module is also removed in this setting.

**3) Real Cloth-Changing Image ReID.** We employ real image-based cloth-changing datasets Real28 [57], VC-Clothes [57], LTCC [48], and PRCC [63] for experiments to validate the effectiveness of GSP module, SC constraints, and also compare our GI-ReID with SOTA cloth-changing ReID methods. In this setting, GSP module and GaitSet are both first pre-trained on gait-specific datasets as described in Sec.3.1 and then fine-tuned on the CC-ReID datasets with the SC constraints  $\mathcal{L}_{MMD}$  &  $\mathcal{L}_{recon.}$  and the basic ReID classification supervision.

## 4.2. Ablation Study

We perform comprehensive ablation studies to demonstrate the effectiveness of proposed Gait-Stream (abbreviated as GS), gait sequence prediction (GSP) module and semantics consistency (SC) constraints in the above-mentioned three experiment settings. All compared schemes use ResNet-50 [14] as ReID backbone.

**Results of General Video ReID.** Table 2 shows the results. We observe that: 1) Thanks to the leverage of gait characteristics through the proposed Gait-Stream (GS), *Baseline + GS (concat)* and *Baseline + GS + SC* outperform *Baseline* by 1.07%/1.29% in mAP respectively, which demonstrates that gait information indeed benefits ReID. 2) We are pleasantly surprised to find that *Baseline + GS + SC* further outperforms *Baseline + GS (concat)* by 0.22% in mAP. This result validates the superiority of our gait utilization manner (*i.e.*, regularization), which makes ReID-Stream not only robust to the gait estimation error, but also computationally efficient (Gait-Stream is not needed in the inference).

Table 2: Performance (%) comparison on the general video ReID dataset MARS [73]. **GS** refers to Gait-Stream and **SC** refers to semantics consistency constraints. Note that ‘concat’ means concatenating ReID vector  $r$  and gait vector  $g$  together for ReID. The backbone is ResNet-50.

Methods	MARS	
	mAP	Rank-1
Baseline	79.12	87.34
Baseline + GS (concat)	80.19	88.16
Baseline + GS + SC (ours)	<b>80.41</b>	<b>88.32</b>

**Results of Imitated Cloth-Changing Video ReID.** To prove that gait indeed could alleviate clothes variation issue, we *imitate* cloth-changing cases for MARS (denoted as CC-MARS). In Table 3, we observe that 1) Disturbed by the synthetic clothing change, *Baseline* suffers from large degradation, 68.52% on CC-MARS vs. 79.12% on raw MARS in mAP. 2) With the assistance of gait, *Baseline+GS*

(*concat*) and *Baseline+GS+SC* improve *Baseline* near 5.0% in mAP. 3) On CC-MARS, the gait ‘concat’ scheme shows a little superiority than ours. We analyse that’s because the ‘concat’ could help ReID more explicitly, especially when meeting changing clothes. But, the ‘concat’ scheme needs maintain Gait-Stream in the inference, leading extra computational cost. 4) As video ReID datasets, it is relatively easy to extract gait features on MARS/CC-MARS.

Table 3: Performance (%) comparison on the imitated (using color jitter) cloth-changing video ReID dataset, termed as CC-MARS. The ReID backbone is ResNet-50.

Methods	CC-MARS	
	mAP	Rank-1
Baseline	68.52	72.31
Baseline + GS (concat)	<b>73.46</b>	<b>79.34</b>
Baseline + GS + SC (ours)	73.13	79.15

**Results of Real Cloth-Changing Image ReID.** We conduct ablation experiments on three cloth-changing datasets Real28, VC-Clothes, and LTCC. Real28 is too small for training, so we train model on VC-Clothes and only test on Real28. In Table 4, we see that 1) All Gait-Stream (GS) related schemes achieve obvious gains (over 2.7% in mAP) over *Baseline*, which demonstrates the effectiveness of using gait to handle cloth-changing issue. 2) With the well-designed GSP module, *Baseline+GS-GSP (concat)* outperforms the ablated scheme *Baseline+GS (concat)* by 3.3%/6.7%/2.3% in mAP on Real28/VC-Clothes/LTCC, which demonstrates GSP’s effectiveness on gait information augmentation. 3) Semantics consistency (SC) constraints performs well in this cloth-changing setting, it helps our scheme GI-ReID achieves the best performance on the most evaluation cases while saving computational cost by discarding Gait-Stream in the inference.

Table 4: Performance (%) comparison on the real image-based cloth-changing datasets Real28, VC-Clothes, LTCC. **GS-GSP** means Gait-Stream (GS) with gait sequence prediction (GSP) module. ReID backbone is ResNet-50. ‘Standard’ is the evaluation setting where the images in the test set with the same identity and camera view are discarded when computing mAP/Rank-1 [48]. Due to the space limitation, we omit ‘Baseline’ on the bottom three schemes.

Methods	Real28		VC-Clothes		LTCC (Standard)	
	mAP	Rank-1	mAP	Rank-1	mAP	Rank-1
Baseline	4.1	6.7	49.1	53.7	23.2	55.1
+ GS (concat)	6.8	7.9	52.3	58.9	26.5	60.0
+ GS-GSP (concat)	10.1	10.8	<b>59.0</b>	63.7	28.8	<b>64.5</b>
+ GS-GSP + SC (ours)	<b>10.4</b>	<b>11.1</b>	57.8	<b>64.5</b>	<b>29.4</b>	63.2

Table 5: Study on the different design choices in the (a)(b) GSP module, and (c) SC constraints of our GI-ReID framework. ‘Cloth-Changing’ setting means that the images with same identity, camera view and clothes are discarded during testing.

(a) Study on the gait prediction length $N$ .					(b) Study on the input gait position $p$ in GSP.					(c) Study on the used losses in SC constraints.				
Methods	LTCC				Methods	LTCC				Methods	LTCC			
	Standard		Cloth-Changing			Standard		Cloth-Changing			Standard		Cloth-Changing	
	mAP	Rank-1	mAP	Rank-1		mAP	Rank-1	mAP	Rank-1		mAP	Rank-1	mAP	Rank-1
Baseline	23.2	55.1	8.1	19.6	Baseline	23.2	55.1	8.1	19.6	Baseline	23.2	55.1	8.1	19.6
N=4	26.9	59.2	8.9	21.7	Arb.	27.1	59.5	9.2	20.5	w/ $\mathcal{L}_{MSE}$	27.5	61.0	9.0	21.4
N=6	28.2	61.9	9.8	22.6	BEGN	28.4	61.2	9.8	22.0	w/o $\mathcal{L}_{recon.}$	28.3	62.7	9.6	22.9
N=8 (ours)	<b>29.4</b>	<b>63.2</b>	<b>10.4</b>	<b>23.7</b>	END	28.1	61.5	9.5	22.4	ours	<b>29.4</b>	<b>63.2</b>	<b>10.4</b>	<b>23.7</b>
N=10	28.4	63.1	10.4	22.8	Mid. (ours)	<b>29.4</b>	<b>63.2</b>	<b>10.4</b>	<b>23.7</b>					
N=12	27.7	60.8	10.0	22.5										

Table 6: Study on the different ReID inference strategies.

Methods	LTCC			
	Standard		Cloth-Changing	
	mAP	Rank-1	mAP	Rank-1
Baseline	23.2	55.1	8.1	19.6
$\tilde{R}$	8.6	21.1	4.3	9.9
$\hat{r} + \hat{g}$	<b>29.8</b>	<b>64.0</b>	<b>10.9</b>	<b>24.4</b>
$\tilde{r} + \tilde{g}$	28.9	63.2	9.7	23.1
$\tilde{r}$	28.1	60.8	9.1	21.3
$r$ (ours)	<u>29.4</u>	<u>63.2</u>	<u>10.4</u>	<u>23.7</u>

### 4.3. Design Choices in Our GI-ReID Framework

We study the different design choices in our GI-ReID framework. We train and test model on the real large-scale cloth-changing ReID dataset LTCC [48].

**Influence of the Length  $N$  of Predicted Gait Sequence.** As shown in Eq-(4) of Sec. 3.1, the output of GSP  $\tilde{R} \in \mathbb{R}^{N \times h \times w}$  is a sequence with  $N$  predicted gait frames. We study the influence of length  $N$  w.r.t the ReID performance. Table 5a shows that when  $N = 8$ , our GI-ReID gets the best performance, achieving a good trade-off between gait prediction error and gait information augmentation.

**Is ‘Middle Frame Input Principle’ Necessary?** As described in Eq-(2) of GSP Sec. 3.1, we employ a position embedder  $P$  and a feature aggregator  $A$  to set up a *middle frame input principle* to reduce the gait prediction ambiguity and difficulty. Here we compare several schemes to show the necessity of such design. **Arb.**: we remove position embedder  $P$ , feature aggregator  $A$ , position loss  $\mathcal{L}_{position}$  for GSP, and take the gait silhouette at *arbitrary* position as input for training. **BEGN** and **END**: we respectively take the gait stance at the *beginning* and the *end* position as input to predict gait sequence during the GSP training. In Table 5b, the scheme **Mid. (ours)** that uses the gait frame at middle position for gait sequence prediction achieves the best performance, outperforming **Arb.** by 2.3% in mAP in the standard setting, which reveals that predicting the gait statuses **before and after** the input middle gait status indeed could reduce prediction difficulty/ambiguity.

**Why Use MMD for Regularization?** For the SC constraints, we draw the gap between the embeded ReID vector

$\hat{r}$  and gait vector  $\hat{g}$  by minimizing MMD through  $\mathcal{L}_{MMD}$ . We study this design in Table 5c and find that when replacing  $\mathcal{L}_{MMD}$  with  $\mathcal{L}_{MSE}$ , the performance of w/  $\mathcal{L}_{MSE}$  drops nearly 2.0% in mAP by ours. That’s because MMD loss is a distribution-level constraint and could better enforce the high-level semantics consistency between dynamic motion gait features and static spatial ReID features. MSE loss is a pixel-wise constraint, and not so suitable to coordinate two modalities of motion gait and RGB feature.

**Is Reconstruction Penalty Necessary?** When removing  $\mathcal{L}_{recon.}$  in Eq-(6), as shown in Table 5c, the scheme w/o  $\mathcal{L}_{recon.}$  is inferior to ours by 1.1%/0.8% in mAP in the two settings, which demonstrates that avoiding information lost caused by feature regularization could enhance the final ReID performance of our GI-ReID framework.

**Which One for ReID Inference?** We compare several cases of using (1) predicted gait sequence  $\tilde{R}$ , (2) aligned features fusion  $\hat{r} + \hat{g}$ , (3) reconstructed features fusion  $\tilde{r} + \tilde{g}$ , and (4) reconstructed ReID vector  $\tilde{r}$  for ReID inference. Table 6 shows that 1) Directly using the predicted gait sequence  $\tilde{R}$  for ReID fails to get satisfactory results, this also indicates that these gait recognition works [3, 9, 8] are not optimal for CC-ReID. 2) Using the well-aligned features fusion  $\hat{r} + \hat{g}$  achieves the best performance, outperforming ours by 0.4%/0.5% in mAP in two settings, but this scheme still needs Gait-Stream in the inference. 3) Using the reconstructed ReID vector  $\tilde{r}$  for inference suffers from information lost and is inferior to ours by 1.3% in mAP in both two settings. 4) Our scheme that using the regularized ReID vector  $r$  achieves the second best performance while saving the computation cost brought by Gait-Stream.

### 4.4. Visualization

**Gait Sequence Prediction Visualization.** We visualize the predicted gait sequence results by GSP module on the cloth-changing ReID datasets in Figure 3. We choose six walking person images from Real28, VC-Clothes, LTCC and PRCC datasets, and respectively present the corresponding predicted gait sequence (length  $N = 8$ ) results. We see that GSP could successfully predict reasonable gait sequence results with continuous phase/motion change. Although there



Table 7: Performance (%) comparisons of our GI-ReID and other competitors on the cloth-changing datasets LTCC [48] and PRCC [63]. ‘†’ means that only identities with clothes changing are used for training. More results in **Supplementary**.

(a) Comparison results on LTCC.

Methods	Standard		Cloth-changing		Standard†		Cloth-changing†	
	Rank-1	mAP	Rank-1	mAP	Rank-1	mAP	Rank-1	mAP
LOMO [35] + NullSpace [67]	34.83	11.92	16.45	6.29	27.59	9.43	13.37	5.34
ResNet-50 + Face [62]	60.44	25.42	22.10	9.44	55.37	22.23	20.68	8.99
PCB [55]	65.11	30.60	23.52	10.03	59.22	26.61	21.93	8.81
HACNN [32]	60.24	26.71	21.59	9.25	57.12	23.48	20.81	8.27
MuDeep [47]	61.86	27.52	23.53	10.23	56.99	24.10	18.66	8.76
LTCC-shape [48]	<u>71.39</u>	<u>34.31</u>	26.15	12.40	<u>66.73</u>	<u>31.29</u>	25.15	11.67
LTCC-shape + Gait-Stream (ours)	—	—	<b>28.86</b>	<b>14.19</b>	—	—	<u>26.41</u>	<b>13.26</b>
Baseline (ResNet-50)	55.14	23.21	19.58	8.10	54.27	21.98	19.14	7.74
GI-ReID (ResNet-50)	63.21	29.44	23.72	10.38	61.39	27.88	22.59	9.87
Baseline (OSNet)	66.07	31.18	23.43	10.56	61.22	27.41	22.97	9.74
GI-ReID (OSNet)	<b>73.59</b>	<b>36.07</b>	28.11	13.17	<b>66.94</b>	<b>33.04</b>	<b>26.71</b>	<u>12.69</u>

(b) Comparison results on PRCC.

Methods	Cross-clothes		
	Rank-1	Rank-10	Rank-20
Shape [1]	11.48	38.66	53.21
LNSCT [60]	15.33	53.87	67.12
HACNN [32]	21.81	59.47	67.45
PCB [55]	22.86	61.24	78.27
SketchNet [66]	17.89	43.70	58.62
Deformable [5]	25.98	71.67	85.31
STN [22]	27.47	69.53	83.22
PRCC-contour [63]	<u>34.38</u>	<u>77.30</u>	<u>88.05</u>
Baseline (ResNet-50)	22.23	61.08	76.44
GI-ReID (ResNet-50)	33.26	75.09	87.44
Baseline (OSNet)	28.70	72.34	85.89
GI-ReID (OSNet)	<b>37.55</b>	<b>82.25</b>	<b>93.76</b>



Figure 3: Six examples of gait sequence prediction results, they come from four cloth-changing ReID datasets Real28, VC-Clothes, LTCC and PRCC. Red boxes mean the input person images and their corresponding predicted middle gait results (see ‘middle frame input principle’).

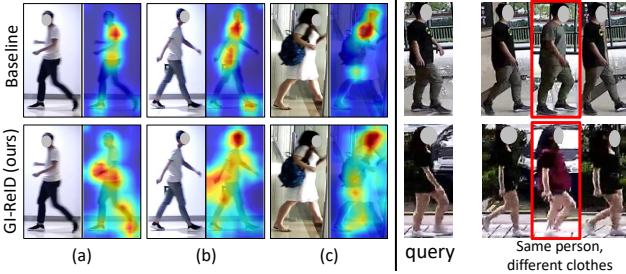


Figure 4: **Left:** three examples of activation maps comparison between baseline and our GI-ReID, which shows GI-ReID not only focuses on people’s clothes, but also pay attention to the holistic human gait and local face; **Right:** Top-3 ranking list of GI-ReID for two query images on Real28 dataset. GI-ReID could identify the same person with different clothes based on the assistance of gait.

exist synthesis errors, the gait information in the prediction are discriminative enough to distinguish different persons, and thus improving CC-ReID performance.

**Feature Map Visualization.** To better understand how our GI-ReID works, we visualize the intermediate activation feature maps of *Baseline* and our GI-ReID for comparison following [76, 74, 24]. On the left of Figure 4, we show three examples of activation maps on Real28, and we observe that the feature maps of *Baseline* have high response mainly on person’s clothes. In contrast, the activation features of our GI-ReID not only have high response on person’s clothes, but also cover the holistic human body structure (gait) and local face information.

## 4.5. Comparison with State-of-the-Arts

The study on cloth-changing ReID is relatively rare [20, 19, 63, 48, 34, 65, 57], and most of them have not released source codes, even the dataset [65]. We compare our GI-ReID with multiple general ReID algorithms, including PCB [55], HACNN [32], MuDeep [47], and specific cloth-changing ReID methods LTCC-shape [48] and PRCC-contour [63]. In Table 7, we observe that 1) Thanks to the utilization of the cloth-independent gait characteristics, our scheme GI-ReID (OSNet) achieves the best performance on LTCC and PRCC, outperforming the second best LTCC-shape [48] by 0.77% and 1.02% in mAP for two cloth-changing settings on LTCC, outperforming PRCC-contour [63] by 3.17% in Rank-1 on PRCC. 2) Our proposed Gait-Stream, as a kind of regularization, could benefit other models, *e.g.*, LTCC-shape. We found that the scheme of *LTCC-shape* + *Gait-Stream* could further obtain 1.79%/1.59% gain in mAP on LTCC. 3) For two cloth-changing settings of LTCC, our scheme GI-ReID (ResNet-50) both achieve obvious gains (2.28%/2.13% in mAP) over the Baseline (ResNet-50), which totally-fair results indicate GI-ReID could eliminate negative impact of clothes changes and learn identity-relevant features. 4) Our method is compatible with existing ReID networks, *e.g.*, built upon the strong ReID-specific network OSNet [76], GI-ReID (OSNet) further achieves gains than GI-ReID (ResNet-50).

## 4.6. Failure Cases Analysis

Due to the large difference on the capture viewpoint and environment between gait and ReID training data, the predicted gait results of GSP are not so accurate (see **Supplementary**) when occlusion, partial, multi-person, *etc.*, existed in the person images, which may hurt CC-ReID performance. That is why we indirectly use gait predictions in a knowledge regularization manner, which makes GI-ReID robust/not sensitive to these failure cases.



## 5. Conclusion

In this paper, we propose to utilize human unique gait to address the cloth-changing ReID problem from a single image. A novel gait-involved two-stream framework GI-ReID is introduced, which takes gait as a regulator with a Gait-Stream (discarded in the inference), to encourage the cloth-agnostic representation learning of mainstream image-based ReID-Stream. To facilitate the gait utilization, a gait sequence prediction (GSP) module and a high-level semantics consistency (SC) constraints are further designed. Extensive experiments on several benchmarks demonstrate the effectiveness and superiority of GI-ReID.

## Supplementary

### 1. Detailed Network Structures of GI-ReID

GI-ReID, as a image-based cloth-changing ReID framework, with gait information as assistance, consists of an auxiliary Gait-Stream and a mainstream ReID-Stream. ReID-Stream can be arbitrary commonly-used network architectures, such as ResNet [14], and also can be some ReID-specific network architectures, such as PCB [55], OSNet [76]. Thus, in this section, we mainly introduce/describe the detailed network architecture of Gait-Stream, which contains two key parts, GSP module for gait information prediction/augmentation and GaitSet [3] for gait features extraction.

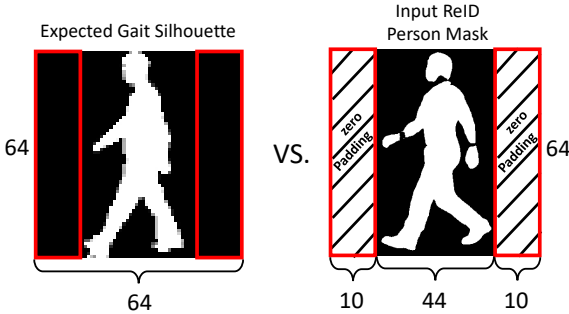


Figure 5: We apply “resize+zero-padding” in the person masks (right) when fine-tuning GSP module on the ReID-specific datasets, because the raw gait training data (left) typically have the height-width ratio of (1:1), which is important/necessary for training GSP to get satisfactory gait prediction results.

**Architecture of Gait Sequence Prediction (GSP) Module:** The proposed GSP module consists of a feature encoder  $E$ , a decoder  $D$ , a position embedder  $P$ , and a feature aggregator  $A$ .

(1). **Encoder  $E$ .** The encoder  $E$  is a CNN with four Conv. layers (filter size =  $4 \times 4$  and stride = 2). The number of filters is increased from  $64 \rightarrow 512$ . Each Conv. layer is followed by a batch-normalization (BN) layer [21] and a

rectified linear unit (ReLU) activation function [43]. In the end, a 100-dimensional feature is obtained through a fully connected (FC) layer.

Note that, when pre-training GSP module on the gait-specific datasets following [3], the input gait silhouette of encoder  $E$  has a size of  $1 \times 64 \times 64$  (height-width ratio is 1:1). We use CASIA-B [3] as training dataset. On the ReID-specific datasets, since the input person images usually have a height-width ratio of 2:1 (e.g., height-256, width-128), we need leverage an operation of “resize+zero-padding” to handle such training data gap, which is pivotal for GSP’s accurate gait sequence prediction. For better understanding, we vividly visualize such process in Figure 5.

(2). **Position Embedder  $P$  and Feature Aggregator  $A$ .** To reduce the gait prediction ambiguity and difficulty of GSP, a position embedder  $P$  and a feature aggregator  $A$  are introduced to integrate the prior information of input middle frame index into the prediction process of GSP. The position embedder  $P$  has a similar structure to that of the encoder  $E$ , but with one more FC layer to regress the 1D position label  $\tilde{p}$ . The feature aggregator  $A$  is inserted between the encoder and the decoder to convert the raw encoded features  $f_S$  into middle-position-aware features  $f_S^{\tilde{p}}$  by taking the embedded middle position information  $\tilde{p}$  into account. With respect to the architecture of  $A$ , it is implemented only by a FC layer, which aims to regress to the aggregated 100-dimension feature  $f_S^{\tilde{p}} \in \mathbb{R}^{100}$  from the **101-dimension** concatenated vector of the raw encoded feature  $f_S \in \mathbb{R}^{100}$  and the embedded middle position prior vector  $\tilde{p} \in \mathbb{R}^1$ .

(3). **Decoder  $D$ .** The structure of the decoder  $D$  is symmetrical to that of the encoder  $E$ . A FC layer along with reshaping is first employed to convert the input 100D feature into the same size as the last feature output of the encoder  $E$ , and then four DeConv. layers are used for up-sampling. A sigmoid activation function is applied in the end, and outputs the gait prediction results with a size of  $N \times 64 \times 64$ , where each channel indicates a predicted gait frame of final results.

**Architecture of GaitSet:** GaitSet [3] is a classic set-based gait recognition network, which takes a set of silhouettes/gait frames as input. After obtaining features from each input silhouette independently using a CNN, *set pooling* is applied to merge features over frames into a set-level feature. This set-level feature is then used for discrimination learning via *horizontal pyramid mapping* (HPM), which aims to extract features of different spatial locations on different scales. We recommend seeing more details from their original paper [3].

### 2. Training Details of our GI-ReID

**Phase-1: Pre-training for GaitSet.** The input is a set of aligned silhouettes in size of  $64 \times 44$ . The silhouettes are directly provided by the datasets and are aligned based on

methods in [56]. The set cardinality in the training is set to be 30. Adam is chosen as an optimizer. The number of scales  $S$  in HPM is set as 5. The margin in separate triplet loss  $\mathcal{L}_{tri}^{sep}$  [3] is set as 0.2. The mini-batch is composed of  $P = 16$  and  $N = 8$  ( $P, N$  respectively mean the number of person identities and input gait frames). We set the number of channels in  $C1$  and  $C2$  as 32, in  $C3$  and  $C4$  as 64 and in  $C5$  and  $C6$  as 128 (following [3]). The learning rate is set to be  $1 \times 10^{-4}$ , and the model is trained for 80 epochs.

### Phase-2: Joint Training for GSP module and GaitSet.

After pre-training GaitSet, we jointly train the proposed gait sequence prediction (GSP) module and GaitSet for Gait-Stream. Specifically, during the joint-training, we also re-use CASIA-B dataset for effective gait prediction training. Following [16], a batch is formed by first randomly sampling  $P$  identities. For each identity, we sample  $N$  continuous gait frames as the ground-truth gait sequence. Then the batch size is  $B = P \times N$ . We set  $P = 4$  and  $N = 8$  (i.e., batch size  $B = P \times N = 32$ ). As presented in the main manuscript, we use the middle one of the ground-truth gait sequence (i.e., the fourth one when  $N = 8$ ) as input for GSP training. We first optimize GSP with the proposed position loss  $\mathcal{L}_{position}$  and prediction loss  $\mathcal{L}_{pred}$  (loss balance is set as 1:1) for 80 epochs, which enables GSP to output reasonable predicted gait sequence results. We train GSP with Adam optimizer [26] with a initial learning rate of  $5 \times 10^{-4}$ . We optimize the Adam optimizer with a weight decay of  $1 \times 10^{-4}$ . The learning rate is decayed by a factor of 0.1 at 40 epoch.

After warming up the GSP module for 80 epochs, we jointly train GSP and GaitSet for extra 160 epochs with initial learning rate as  $5 \times 10^{-4}$ . We also use Adam optimizer [26] for optimization with a weight decay of  $1 \times 10^{-4}$ , the learning rate is decayed by a factor of 0.5 at 40, 80, and 120 epochs. When jointly training GSP and GaitSet, excluding the GSP-related position loss  $\mathcal{L}_{position}$  and prediction loss  $\mathcal{L}_{pred}$ , we further use *separate triplet loss*  $\mathcal{L}_{tri}^{sep}$  for training, which is introduced in details in GaitSet [3], and we also set the loss weight as 1.0 for this supervision.

### Phase-3: Joint Training for Gait-Stream and ReID-Stream.

When we jointly training Gait-Stream and ReID-Stream on the ReID datasets, Gait-Stream is also fine-tuned/learnable. Since the full gait sequence ground truth are not available for ReID-specific datasets, we adjust the original prediction loss  $\mathcal{L}_{pred}$  in GSP by only calculating L1 distance between the single input person mask and the middle frame result of the entire predicted gait sequence.

On the large-scale cloth-changing datasets VC-Clothes [57], LTCC [48], and PRCC [63], we set training batch size as  $B = 80 = P \times N = 10 \times 8$ . Both of Gait-Stream (including GSP and GaitSet) and ReID-Stream use Adam optimizer [26] for optimization, where the initial learning rate for Gait-Stream is  $1 \times 10^{-5}$ , for ReID-Stream

### Algorithm 1 Training Process of GI-ReID

---

```

1: Input: gait dataset  $\mathcal{G}$  (e.g., CASIA-B [3]), ReID dataset  $\mathcal{R}$  (e.g.,
   LTCC [48]). Learning rate is simply denoted as  $\eta$ . The entire GI-
   ReID framework consists of GSP module  $GSP_\theta$ , GaitSet (GS)  $GS_\phi$ ,
   SC constraints related FC layers  $SC_\psi$ , and ReID-Stream backbone
    $ReID_\omega$ .
2: Output: inference ReID vector  $r$ .
3: ### Phase-1: Pre-training for GaitSet
4: for  $epoch = 1$  to 80 do
5:   Sample  $P \times N = 16 \times 8$  samples from gait training set  $\mathcal{G}$ .
6:    $\mathcal{L}_{total} = \mathcal{L}_{tri}^{sep}$  // Use the separate triplet loss as objective
   function [3].
7:    $\phi = \phi - \eta \nabla_\phi \mathcal{L}_{tri}^{sep}$  // Update GaitSet (GS)  $GS_\phi$ .
8: end for
9: ### Phase-2: Joint Training for GSP module and GaitSet
10: for  $epoch = 1$  to 80 do
11:   Sample  $P \times N = 4 \times 8$  samples from gait training set  $\mathcal{G}$ .
12:    $\mathcal{L}_{total} = \mathcal{L}_{position} + \mathcal{L}_{pred}$  // Use the proposed position loss
   and prediction loss as objective functions.
13:    $\theta = \theta - \eta \nabla_\theta \mathcal{L}_{total}$  // Warm up GSP module  $GSP_\theta$ .
14: end for
15: for  $epoch = 1$  to 160 do
16:   Sample  $P \times N = 4 \times 8$  samples from gait training set  $\mathcal{G}$ .
17:    $\mathcal{L}_{total} = \mathcal{L}_{position} + \mathcal{L}_{pred} + \mathcal{L}_{tri}^{sep}$  // Use the position loss,
   prediction loss, and separate triplet loss as objective functions.
18:    $(\theta, \phi) = (\theta, \phi) - \eta \nabla_{(\theta, \phi)} \mathcal{L}_{total}$  // Jointly update GSP module
    $GSP_\theta$  and GaitSet (GS)  $GS_\phi$ .
19: end for
20: ### Phase-3: Joint Training for Gait-Stream and ReID-Stream
21: for  $epoch = 1$  to 240 do
22:   Sample  $P \times N = 10 \times 8$  samples from ReID training set  $\mathcal{R}$ .
23:    $\mathcal{L}_{total} = 0.1 * \mathcal{L}_{position} + 0.1 * \mathcal{L}_{pred} + 0.1 * \mathcal{L}_{tri}^{sep} + \mathcal{L}_{cla} +$ 
    $\mathcal{L}_{tri}^{HM} + 0.5 * \mathcal{L}_{MMD} + 0.5 * \mathcal{L}_{recon}$ . //
   Total objective functions consists of the position loss, prediction
   loss, separate triplet loss (for Gait-Stream), and the classification
   loss, triplet loss (with hard-mining, HM) (for ReID-Stream), and
   the MMD loss, reconstruction loss (SC constraints).
24:    $(\theta, \phi, \psi, \omega) = (\theta, \phi, \psi, \omega) - \eta \nabla_{(\theta, \phi, \psi, \omega)} \mathcal{L}_{total}$  // Jointly update
   GSP module  $GSP_\theta$ , GaitSet (GS)  $GS_\phi$ , SC constraints related FC
   embedding layers  $SC_\psi$ , and ReID-Stream backbone  $ReID_\omega$ .
25: end for

```

---

is  $5 \times 10^{-4}$ . We optimize two Adam optimizers for Gait-Stream and ReID-Stream with a weight decay of  $1 \times 10^{-5}$  for total 240 epochs. The learning rate is decayed by a factor of 0.1 at 80 and 160 epochs for ReID-Stream, while no learning rate decay for Gait-Stream. For the losses usage, we adopt the widely-adopted classification loss  $\mathcal{L}_{cla}$  [55, 10], and triplet loss with batch hard mining  $\mathcal{L}_{tri}^{HM}$  [16]) as basic optimization objectives for ReID-Stream training, and we set these two loss weights as 1.0. Besides, for the Gait-Stream related losses, including  $\mathcal{L}_{position}$ ,  $\mathcal{L}_{pred}$ ,  $\mathcal{L}_{tri}^{sep}$ , we set all their loss weights as 0.1. For the semantics consistency (SC) constraints related FC embedding layers, we merge their learnable parameters into ReID-Stream's optimization, and set the balance weights for MMD loss  $\mathcal{L}_{MMD}$  and reconstruction penalty  $\mathcal{L}_{recon}$  as 0.5. The pseudo code of the entire training process of our GI-ReID is given in Algorithm 1.

### 3. Details of Datasets

We use one widely-used video ReID dataset MARS [73], and four image-based cloth-changing ReID datasets Real28 [57], VC-Clothes [57], LTCC [48], PRCC [63] to perform experiments. In Table 8, we present the detailed information about these ReID datasets.

Table 8: Brief introduction/comparison of datasets.

	MARS	Real28	VC-Clothes	LTCC	PRCC
Category	Video	Image	Image	Image	Image
Photo Style	Real	Real	Synthetic	Real	Real
Scale	Large	Small	Large	Large	Large
Cloth Change	No	Yes	Yes	Yes	Yes
Identities	1,261	28	512	152	221
Samples	20,715	4,324	19,060	17,138	33,698
Cameras	6	4	4	N/A	3
Usage	Train&Test	Test	Train&Test	Train&Test	Train&Test

MARS is a popular dataset for video-based person ReID. There are 20,715 track-lets come from 1,261 pedestrians who are captured by at least 2 cameras. We use the train/test split protocol defined in [73].

Real28, VC-Clothes, LTCC and PRCC are all newly released image datasets for cloth-changing ReID [57, 48, 63].

Real28 is a **small** real-scenario dataset, which is collected in 3 different days (with different clothing) by 4 cameras. It consists of totally 4,324 images from 28 different identities with 2 indoor scenes and 2 outdoors. Similar to [57], since the size of Real28 is not big enough for training deep learning models, we just use it for evaluation. There are totally 336 images in the query and 3,988 images in the gallery.

VC-Clothes is a **synthetic** dataset where images are rendered by the Grand Theft Auto V (GTA5). It has 512 identities, 4 scenes (cameras) and on average 9 images/scenes for each identity and a total number of 19,060 images. Following [57], we equally split the dataset by identities: 256 identities for training and the other 256 for testing. We randomly chose 4 images per person from each camera as query, and have the other images serve as gallery images. Eventually, we get totally 9,449 images in the training, 1,020 images as queries and 8,591 others in the gallery.

LTCC is a **large-scale real-scenario** cloth-changing dataset, which contains 17,138 person images of 152 identities. On average, there are 5 different clothes for each cloth-changing person, with the numbers of outfit changes ranging from 2 to 14. Following [48], we split the LTCC dataset into training and testing sets. The training set consists of 77 identities, where 46 people have cloth changes and the rest of 31 people wear the same outfits during the recording. Similarly, the testing set contains 45 people with changing clothes and 30 people wearing the same outfits.

PRCC is also a **large-scale real-scenario** cloth-changing dataset, recently published by Yang *et al.* [63]. It consists of 221 identities with three camera views *Camera*

*A*, *Camera B*, and *Camera C*. Each person in Cameras A and B is wearing the same clothes, but the images are captured in different rooms. For Camera C, the person wears different clothes, and the images are captured in a different day. The images in the PRCC dataset include not only clothing changes for the same person across different camera views but also other variations, *e.g.* changes in illumination, occlusion, pose and viewpoint. In summary, nearly 50 images exists for each person in each camera view. Therefore, approximately 152 images of each person are included in the dataset, for 33,698 images in total.

Following [63], we split the PRCC dataset into a training set and a testing set. The training set consists of 150 people, and the testing set consists of 71 people, with no overlap between them in terms of identities. The testing set was further divided into a gallery set and a probe set. For each identity in the testing set, we chose one image in *Camera view A* to form the gallery set for a single-shot matching. All images in *Camera views B* and *Camera C* were used for the probe set. Specifically, the person matching between Camera views A and B was performed without clothing changes, whereas the matching between Camera views A and C was cross-clothes matching. The results were assessed in terms of the cumulated matching characteristics, specifically, the Rank-1, Rank-10, and Rank-20 matching accuracy.

Table 9: Performance (%) comparison on the cloth-changing dataset LTCC. Such experiment aims to show that our GI-ReID can bring gains because of the exploration of gait information, rather than simply introducing human masks. The ReID backbone is ResNet-50.

Methods	LTCC (Cloth-Changing)	
	mAP	Rank-1
Baseline (ResNet-50)	8.10	19.58
MaskReID	7.04	17.92
GI-ReID (ours)	<b>10.38</b>	<b>23.72</b>

### 4. More Experimental Analysis Results

#### Difference Discussion with Mask-guided ReID Methods.

We believe that our GI-ReID could successfully address the cloth-changing ReID problem from a single image is indeed because we effectively leverage the gait information, instead of the introduction of human body mask. To prove that, we additionally design a scheme *MaskReID* that directly takes the person RGB-Mask pair as input to ReID model (following [51, 4]), and compare it with our GI-ReID on the cloth-changing ReID dataset LTCC. ResNet-50 is taken as ReID backbone for all schemes for comparison fairness. As shown in Table 9, we found that *MaskReID* is even inferior to the baseline scheme *Baseline (ResNet-50)* by 1.06% in mAP under the cloth-changing setting. Our

analysis is because directly using mask to remove the background clutters in pixel-level will make ReID model more rely on the appearance/clothes color information, which is unexpected and unreliable for cloth-changing ReID, and thus leads to a performance drop.

**Pure Gait Recognition Works are not Optimal For Cloth-Changing ReID.** As we have discussed in details in the main manuscripts, directly using gait sequences/masks for identity matching is not optimal for cloth-changing ReID problem, especially in the image-based ReID scenarios. Experimentally, we compare the proposed GI-ReID with two popular pure gait recognition works, GaitSet [3] and PA-GCR [61]. GaitSet needs a set/sequence of person masks as input, but recently-released cloth-changing ReID datasets are image datasets that lack of continuous frames for the same person. Thus, we duplicate the only available single one person mask to a set as input to approximately apply GaitSet into image-based CC-ReID task. As shown in Table 10, these pure gait recognition works of GaitSet [3] and PA-GCR [61] are both inferior to the baseline scheme *Baseline (ResNet-50)* in mAP under the cloth-changing setting, which indicates that simply/directly using gait biometric for person matching can not work well for cloth-changing ReID, our gait prediction and regularization idea seems a right way to solve CC-ReID, especially for the image-based CC-ReID.

Table 10: Performance (%) comparison on the cloth-changing dataset LTCC. Such experiment aims to show that these pure gait recognition works can not work well for CC-ReID.

Methods	LTCC (Cloth-Changing)	
	mAP	Rank-1
Baseline (ResNet-50)	8.10	19.58
GaitSet [3]	2.14	7.22
PA-GCR [61]	3.36	9.01
GI-ReID (ours)	<b>10.38</b>	<b>23.72</b>

## 5. Study on Failure Cases

As we described in the main manuscript, since the existed large difference on the capture viewpoint and environment between gait and ReID training data, the predicted results of gait sequence prediction (GSP) module are not so accurate when occlusion, partial, multi-person, *etc*, existed in the person images. As shown in Figure 6, GSP gives unsatisfactory gait prediction results, where large estimation errors exist in the predicted gait frames, which will hurt the ReID performance. That is why we **indirectly** use gait prediction results in a two-stream knowledge regularization manner, which makes our GI-ReID robust/less sensitive to these failure cases.

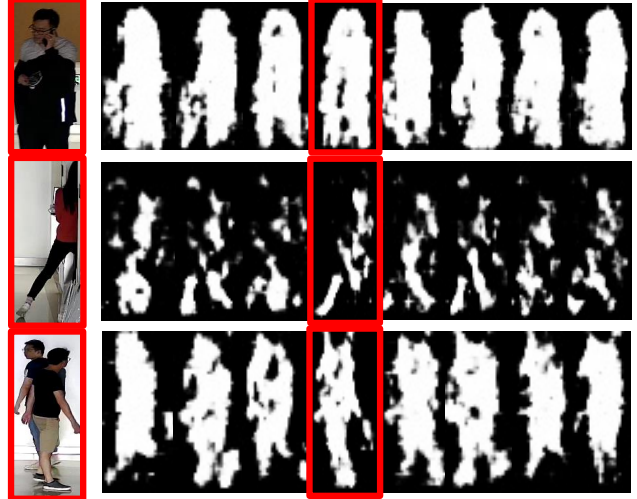


Figure 6: Failure cases of gait sequence prediction (GSP).

## 6. Comparison with State-of-the-Arts (Complete version)

To save space, we only present the latest approaches in the main manuscripts, and here we show comparisons with more approaches and more evaluation settings on LTCC (Table 11) and PRCC datasets (Table 12).

From the comparison results on PRCC that are shown in Table 12, we observe that 1) Although person ReID with no clothing change (*i.e.* “Same Clothes” in the Table 12) is not the purpose in our work, our method GI-ReID can still achieve an accuracy of 85.97% in Rank-1, which is better than that of all hand-crafted features with metric learning methods and most deep learning methods. 2) When the input images are RGB images without clothing changes, Alexnet [31], VGG16 [50], HA-CNN [32], and PCB [55] all achieve good performance, but they have a sharp performance drop when a clothing change occurs, illustrating the challenge of person ReID when a person dresses differently. Therefore, the application of existing person ReID methods is not straightforward in this scenario. In contrast, our GI-ReID that leverages gait information is beneficial to learn the clothing invariant feature, which makes our method achieve satisfactory performance 37.55% in Rank-1 even under the cloth-changing scenario.

## References

- [1] Serge Belongie, Jitendra Malik, and Jan Puzicha. Shape matching and object recognition using shape contexts. *IEEE TPAMI*, 24(4):509–522, 2002. 8, 13
- [2] Cassandra Carley, Ergys Ristani, and Carlo Tomasi. Person re-identification from gait using an autocorrelation network. In *CVPRW*, pages 0–0, 2019. 3
- [3] Hanqing Chao, Yiwei He, Junping Zhang, and Jianfeng Feng. Gaitset: Regarding gait as a set for cross-view gait



Table 11: Performance (%) comparisons of our GI-ReID and other competitors on the cloth-changing dataset LTCC [48]. ‘Standard’ and ‘Cloth-changing’ respectively mean the standard setting and cloth-changing setting as mentioned in our main manuscript. ‘(Image)’ or ‘(Parsing)’ represents that the input data is the person image or the body parsing image. ‘†’ means the setting that only identities with clothes changing are used for training.

Methods	Standard		Cloth-changing		Standard <sup>†</sup>		Cloth-changing <sup>†</sup>	
	Rank-1	mAP	Rank-1	mAP	Rank-1	mAP	Rank-1	mAP
LOMO [35] + KISSME [28]	26.57	9.11	10.75	5.25	19.47	7.37	8.32	4.37
LOMO [35] + XQDA [35]	25.35	9.54	10.95	5.56	22.52	8.21	10.55	4.95
LOMO [35] + NullSpace [67]	34.83	11.92	16.45	6.29	27.59	9.43	13.37	5.34
ResNet-50 (Image) [14]	58.82	25.98	20.08	9.02	57.20	22.82	20.68	8.38
ResNet-50 (Parsing) [14]	19.87	6.64	7.51	3.75	18.86	6.16	6.28	3.46
PCB (Parsing) [55]	27.38	9.16	9.33	4.50	25.96	7.77	10.54	4.04
ResNet-50 + Face [62]	60.44	25.42	22.10	9.44	55.37	22.23	20.68	8.99
PCB [55]	65.11	30.60	23.52	10.03	59.22	26.61	21.93	8.81
HACNN [32]	60.24	26.71	21.59	9.25	57.12	23.48	20.81	8.27
MuDeep [47]	61.86	27.52	23.53	10.23	56.99	24.10	18.66	8.76
Face [62]	60.44	25.42	22.10	9.44	55.37	22.23	20.68	8.99
LTCC-shape [48]	71.39	34.31	26.15	12.40	66.73	31.29	25.15	11.67
LTCC-shape + Gait-Stream (ours)	–	–	<b>28.86</b>	<b>14.19</b>	–	–	<u>26.41</u>	<b>13.26</b>
Baseline (ResNet-50)	55.14	23.21	19.58	8.10	54.27	21.98	19.14	7.74
GI-ReID (ResNet-50) (ours)	63.21	29.44	23.72	10.38	61.39	27.88	22.59	9.87
Baseline (OSNet)	66.07	31.18	23.43	10.56	61.22	27.41	22.97	9.74
GI-ReID (OSNet) (ours)	<b>73.59</b>	<b>36.07</b>	<u>28.11</u>	<u>13.17</u>	<b>66.94</b>	<b>33.04</b>	<b>26.71</b>	<u>12.69</u>

Table 12: Performance (%) comparisons of our GI-ReID and other competitors on the cloth-changing dataset PRCC [63]. “RGB” means the inputs of the model are RGB images; “Sketch” means the inputs of the model are contour sketch images

Methods	Cameras A and C (Cross-Clothes)			Cameras A and B (Same Clothes)		
	Rank-1	Rank-10	Rank-20	Rank-1	Rank-10	Rank-20
LBP [45] + KISSME [29]	18.71	58.09	71.40	39.03	76.18	86.91
HOG [6] + KISSME [29]	17.52	49.52	63.55	36.02	68.83	80.49
LBP [45] + HOG [6] + KISSME [29]	17.66	54.07	67.85	47.73	81.88	90.54
LOMO [36] + KISSME [29]	18.55	49.81	67.27	47.40	81.42	90.38
LBP [45] + XQDA [36]	18.25	52.75	61.98	40.66	77.74	87.44
HOG [6] + XQDA [36]	22.11	57.33	69.93	42.32	75.63	85.38
LBP [45] + HOG [6] + XQDA [36]	23.71	62.04	74.49	54.16	84.11	91.21
LOMO [36] + XQDA [36]	14.53	43.63	60.34	29.41	67.24	80.52
Shape [1]	11.48	38.66	53.21	23.87	68.41	76.32
LNSCT [60]	15.33	53.87	67.12	35.54	69.56	82.37
Alexnet [31] (RGB)	16.33	48.01	65.87	63.28	91.70	94.73
VGG16 [50] (RGB)	18.21	46.13	60.76	71.39	95.89	98.68
HA-CNN [32] (RGB)	21.81	59.47	67.45	82.45	98.12	99.04
PCB [55] (RGB)	22.86	61.24	78.27	<b>86.88</b>	<u>98.79</u>	<u>99.62</u>
Alexnet [31] (Sketch)	14.94	57.68	75.40	38.00	82.15	91.91
VGG16 [50] (Sketch)	18.79	66.01	81.27	54.00	91.33	96.73
HA-CNN [32] (Sketch)	20.45	63.87	79.58	58.63	90.45	95.78
PCB [55] (Sketch)	22.48	61.07	77.05	57.36	92.12	96.72
SketchNet [66] (Sketch+RGB)	17.89	43.70	58.62	64.56	95.09	97.84
Face [59]	2.97	9.85	13.52	4.75	13.40	45.54
Deformable Conv. [5]	25.98	71.67	85.31	61.87	92.13	97.65
STN [22]	27.47	69.53	83.22	59.21	91.43	96.11
PRCC-contour [63]	34.38	77.30	88.05	64.20	92.62	96.65
PRCC-contour + Gait-Stream (ours)	<u>36.19</u>	<u>79.93</u>	<u>91.67</u>	–	–	–
Baseline (ResNet-50)	22.23	61.08	76.44	75.81	97.34	98.95
GI-ReID (ResNet-50) (ours)	33.26	75.09	87.44	78.95	97.89	99.11
Baseline (OSNet)	28.70	72.34	85.89	83.68	98.24	99.26
GI-ReID (OSNet) (ours)	<b>37.55</b>	<b>82.25</b>	<b>93.76</b>	<u>85.97</u>	<b>98.82</b>	<b>99.72</b>

- recognition. In *AAAI*, volume 33, pages 8126–8133, 2019. 2, 3, 4, 7, 9, 10, 12
- [4] Di Chen, Shanshan Zhang, Wanli Ouyang, Jian Yang, and Ying Tai. Person search via a mask-guided two-stream cnn model. In *ECCV*, pages 734–750, 2018. 11
- [5] Jifeng Dai, Haozhi Qi, Yuwen Xiong, Yi Li, Guodong Zhang, Han Hu, and Yichen Wei. Deformable convolutional networks. In *ICCV*, pages 764–773, 2017. 8, 13
- [6] Navneet Dalal and Bill Triggs. Histograms of oriented gradients for human detection. 2005. 13
- [7] Carl Doersch. Tutorial on variational autoencoders. *arXiv preprint arXiv:1606.05908*, 2016. 4
- [8] Omar Elharrouss, Noor Almaadeed, Somaya Al-Maadeed, and Ahmed Bouridane. Gait recognition for person re-identification. *The Journal of Supercomputing*, pages 1–20, 2020. 3, 7
- [9] Chao Fan, Yunjie Peng, Chunshui Cao, Xu Liu, Saihui Hou, Jiannan Chi, Yongzhen Huang, Qing Li, and Zhiqiang He. Gaitpart: Temporal part-based model for gait recognition. In *CVPR*, June 2020. 2, 3, 7
- [10] Yang Fu, Yunchao Wei, Yuqian Zhou, Honghui Shi, Gao Huang, Xinchao Wang, Zhiqiang Yao, and Thomas Huang. Horizontal pyramid matching for person re-identification. In *AAAI*, volume 33, pages 8295–8302, 2019. 2, 4, 10
- [11] Yixiao Ge, Zhuowan Li, Haiyu Zhao, et al. Fd-gan: Pose-guided feature distilling gan for robust person re-identification. In *NeurIPS*, 2018. 2
- [12] Arthur Gretton, Karsten M Borgwardt, Malte J Rasch, Bernhard Schölkopf, and Alexander Smola. A kernel two-sample test. *The Journal of Machine Learning Research*, 13(1):723–773, 2012. 5
- [13] Vincent Le Guen and Nicolas Thome. Disentangling physical dynamics from unknown factors for unsupervised video prediction. In *CVPR*, pages 11474–11484, 2020. 4
- [14] Kaiming He, Xiangyu Zhang, Shaoqing Ren, et al. Deep residual learning for image recognition. In *CVPR*, 2016. 4, 6, 9, 13
- [15] Lingxiao He, Jian Liang, Haiqing Li, and Zhenan Sun. Deep spatial feature reconstruction for partial person re-identification: Alignment-free approach. In *CVPR*, 2018. 2
- [16] Alexander Hermans, Lucas Beyer, and Bastian Leibe. In defense of the triplet loss for person re-identification. *arXiv preprint arXiv:1703.07737*, 2017. 4, 10
- [17] Geoffrey Hinton, Oriol Vinyals, and Jeff Dean. Distilling the knowledge in a neural network. *arXiv preprint arXiv:1503.02531*, 2015. 5
- [18] Jun-Ting Hsieh, Bingbin Liu, De-An Huang, Li F Fei-Fei, and Juan Carlos Niebles. Learning to decompose and disentangle representations for video prediction. In *NeurIPS*, pages 517–526, 2018. 4
- [19] Yan Huang, Qiang Wu, Jingsong Xu, and Yi Zhong. Celebrities-reid: A benchmark for clothes variation in long-term person re-identification. In *IJCNN*, pages 1–8. IEEE, 2019. 1, 2, 8
- [20] Yan Huang, Jingsong Xu, Qiang Wu, Yi Zhong, Peng Zhang, and Zhaoxiang Zhang. Beyond scalar neuron: Adopting vector-neuron capsules for long-term person re-identification. *TCSVT*, 2019. 1, 2, 8
- [21] Sergey Ioffe and Christian Szegedy. Batch normalization: Accelerating deep network training by reducing internal covariate shift. *ICML*, 2015. 9
- [22] Max Jaderberg, Karen Simonyan, Andrew Zisserman, et al. Spatial transformer networks. In *NeurIPS*, pages 2017–2025, 2015. 8, 13
- [23] Xin Jin, Cuiling Lan, Wenjun Zeng, and Zhibo Chen. Uncertainty-aware multi-shot knowledge distillation for image-based object re-identification. In *AAAI*, 2020. 1, 2
- [24] Xin Jin, Cuiling Lan, Wenjun Zeng, Zhibo Chen, and Li Zhang. Style normalization and restitution for generalizable person re-identification. In *CVPR*, pages 3143–3152, 2020. 1, 8
- [25] Xin Jin, Cuiling Lan, Wenjun Zeng, Guoqiang Wei, and Zhibo Chen. Semantics-aligned representation learning for person re-identification. In *AAAI*, 2020. 1, 2
- [26] Diederik P Kingma and Jimmy Ba. Adam: A method for stochastic optimization. In *ICLR*, 2014. 10
- [27] Alexander Kirillov, Yuxin Wu, Kaiming He, and Ross Girshick. Pointrend: Image segmentation as rendering. In *CVPR*, pages 9799–9808, 2020. 4
- [28] Aniket Kittur, Ed H. Chi, and Bongwon Suh. Crowdsourcing user studies with mechanical turk. 2008. 13
- [29] Martin Koestinger, Martin Hirzer, Paul Wohlhart, Peter M Roth, and Horst Bischof. Large scale metric learning from equivalence constraints. In *CVPR*, pages 2288–2295. IEEE, 2012. 13
- [30] Zoe Kourtzi and Nancy Kanwisher. Activation in human mt/mst by static images with implied motion. *Journal of cognitive neuroscience*, 12(1):48–55, 2000. 2
- [31] Alex Krizhevsky, Ilya Sutskever, and Geoffrey E Hinton. Imagenet classification with deep convolutional neural networks. *Communications of the ACM*, 60(6):84–90, 2017. 12, 13
- [32] Wei Li, Xiatian Zhu, and Shaogang Gong. Harmonious attention network for person re-identification. In *CVPR*, 2018. 8, 12, 13
- [33] Xiang Li, Yasushi Makihara, Chi Xu, Yasushi Yagi, and Mingwu Ren. Gait recognition via semi-supervised disentangled representation learning to identity and covariate features. In *CVPR*, pages 13309–13319, 2020. 3
- [34] Yu-Jhe Li, Zhengyi Luo, Xinshuo Weng, and Kris M Kitani. Learning shape representations for clothing variations in person re-identification. *arXiv preprint arXiv:2003.07340*, 2020. 2, 3, 8
- [35] S. Liao, Y. Hu, X. Zhu, and S. Z. Li. Person re-identification by local maximal occurrence representation and metric learning. In *CVPR*, 2015. 8, 13
- [36] Shengcai Liao, Yang Hu, Xiangyu Zhu, and Stan Z Li. Person re-identification by local maximal occurrence representation and metric learning. In *CVPR*, 2015. 13
- [37] Yu-Lun Liu, Yi-Tung Liao, Yen-Yu Lin, and Yung-Yu Chuang. Deep video frame interpolation using cyclic frame generation. In *AAAI*, volume 33, pages 8794–8802, 2019. 4
- [38] Zheng Liu, Zhaoxiang Zhang, Qiang Wu, and Yunhong Wang. Enhancing person re-identification by integrating gait biometric. *Neurocomputing*, 168:1144–1156, 2015. 3

- [39] Yasushi Makihara, Atsuyuki Suzuki, Daigo Muramatsu, Xiang Li, and Yasushi Yagi. Joint intensity and spatial metric learning for robust gait recognition. In *CVPR*, pages 5705–5715, 2017. 3
- [40] Simone Meyer, Oliver Wang, Henning Zimmer, Max Grosse, and Alexander Sorkine-Hornung. Phase-based frame interpolation for video. In *CVPR*, pages 1410–1418, 2015. 4
- [41] Jiaxu Miao, Yu Wu, Ping Liu, Yuhang Ding, and Yi Yang. Pose-guided feature alignment for occluded person re-identification. In *ICCV*, pages 542–551, 2019. 2
- [42] Daigo Muramatsu, Akira Shiraishi, Yasushi Makihara, Md Zassim Uddin, and Yasushi Yagi. Gait-based person recognition using arbitrary view transformation model. *TIP*, 24(1):140–154, 2014. 3
- [43] Vinod Nair and Geoffrey E Hinton. Rectified linear units improve restricted boltzmann machines. In *ICML*, 2010. 9
- [44] Simon Niklaus and Feng Liu. Context-aware synthesis for video frame interpolation. In *CVPR*, pages 1701–1710, 2018. 4
- [45] Timo Ojala, Matti Pietikäinen, and David Harwood. A comparative study of texture measures with classification based on featured distributions. *Pattern recognition*, 29(1):51–59, 1996. 13
- [46] Xuelin Qian, Yanwei Fu, Wenxuan Wang, et al. Pose-normalized image generation for person re-identification. In *ECCV*, 2018. 1, 2
- [47] Xuelin Qian, Yanwei Fu, Tao Xiang, Yu-Gang Jiang, and Xiangyang Xue. Leader-based multi-scale attention deep architecture for person re-identification. *TPAMI*, 2019. 8, 13
- [48] Xuelin Qian, Wenxuan Wang, Li Zhang, Fangrui Zhu, Yanwei Fu, Tao Xiang, Yu-Gang Jiang, and Xiangyang Xue. Long-term cloth-changing person re-identification. *WACV*, 2020. 1, 2, 3, 5, 6, 7, 8, 10, 11, 13
- [49] Sara Sabour, Nicholas Frosst, and Geoffrey E Hinton. Dynamic routing between capsules. In *NeurIPS*, pages 3856–3866, 2017. 3
- [50] Karen Simonyan and Andrew Zisserman. Very deep convolutional networks for large-scale image recognition. *arXiv preprint arXiv:1409.1556*, 2014. 12, 13
- [51] Chunfeng Song, Yan Huang, Wanli Ouyang, and Liang Wang. Mask-guided contrastive attention model for person re-identification. In *CVPR*, 2018. 11
- [52] Chi Su, Jianing Li, Shiliang Zhang, et al. Pose-driven deep convolutional model for person re-identification. In *ICCV*, 2017. 1, 2
- [53] Xiaoxiao Sun and Liang Zheng. Dissecting person re-identification from the viewpoint of viewpoint. *arXiv preprint arXiv:1812.02162*, 2018. 2
- [54] Xiaoxiao Sun and Liang Zheng. Dissecting person re-identification from the viewpoint of viewpoint. In *CVPR*, pages 608–617, 2019. 1
- [55] Yifan Sun, Liang Zheng, Yi Yang, Qi Tian, and Shengjin Wang. Beyond part models: Person retrieval with refined part pooling (and a strong convolutional baseline). In *ECCV*, pages 480–496, 2018. 2, 4, 8, 9, 10, 12, 13
- [56] Noriko Takemura, Yasushi Makihara, Daigo Muramatsu, Tomio Echigo, and Yasushi Yagi. Multi-view large population gait dataset and its performance evaluation for cross-view gait recognition. *IPSP Transactions on Computer Vision and Applications*, 10(1):4, 2018. 10
- [57] Fangbin Wan, Yang Wu, Xuelin Qian, Yixiong Chen, and Yanwei Fu. When person re-identification meets changing clothes. In *CVPRW*, pages 830–831, 2020. 1, 2, 3, 5, 6, 8, 10, 11
- [58] Guanshuo Wang, Yufeng Yuan, Xiong Chen, et al. Learning discriminative features with multiple granularities for person re-identification. In *ACM MM*, pages 274–282, 2018. 2, 4
- [59] Yandong Wen, Kaipeng Zhang, Zhifeng Li, and Yu Qiao. A discriminative feature learning approach for deep face recognition. In *ECCV*, pages 499–515. Springer, 2016. 13
- [60] Xiaohua Xie, Jianhuang Lai, and Wei-Shi Zheng. Extraction of illumination invariant facial features from a single image using nonsubsampled contourlet transform. *Pattern Recognition*, 43(12):4177–4189, 2010. 8, 13
- [61] Chi Xu, Yasushi Makihara, Xiang Li, Yasushi Yagi, and Jianfeng Lu. Gait recognition from a single image using a phase-aware gait cycle reconstruction network. *eccv 2020*. 3, 12
- [62] Jia Xue, Zibo Meng, Karthik Katipally, Haibo Wang, and Kees van Zon. Clothing change aware person identification. In *CVPRW*, pages 2112–2120, 2018. 2, 8, 13
- [63] Qize Yang, Ancong Wu, and Wei-Shi Zheng. Person re-identification by contour sketch under moderate clothing change. *TPAMI*, 2019. 1, 2, 3, 5, 6, 8, 10, 11, 13
- [64] Jingwen Ye, Yixin Ji, Xinchao Wang, Kairi Ou, Dapeng Tao, and Mingli Song. Student becoming the master: Knowledge amalgamation for joint scene parsing, depth estimation, and more. In *CVPR*, pages 2829–2838, 2019. 5
- [65] Shijie Yu, Shihua Li, Dapeng Chen, Rui Zhao, Junjie Yan, and Yu Qiao. Cocos: A large-scale clothes changing person dataset for re-identification. In *CVPR*, pages 3400–3409, 2020. 1, 2, 3, 8
- [66] Hua Zhang, Si Liu, Changqing Zhang, Wenqi Ren, Rui Wang, and Xiaochun Cao. Sketchnet: Sketch classification with web images. In *CVPR*, pages 1105–1113, 2016. 8, 13
- [67] Li Zhang, Tao Xiang, and Shaogang Gong. Learning a discriminative null space for person re-identification. In *CVPR*, 2016. 8, 13
- [68] Li Zhang, Tao Xiang, and Shaogang Gong. Learning a discriminative null space for person re-identification. In *CVPR*, 2016. 1
- [69] Peng Zhang, Qiang Wu, Jingsong Xu, and Jian Zhang. Long-term person re-identification using true motion from videos. In *WACV*, pages 494–502. IEEE, 2018. 3
- [70] Ying Zhang, Tao Xiang, Timothy M Hospedales, and Huchuan Lu. Deep mutual learning. In *CVPR*, 2018. 5
- [71] Zhizheng Zhang, Cuiling Lan, Wenjun Zeng, et al. Densely semantically aligned person re-identification. In *CVPR*, 2019. 2
- [72] Haiyu Zhao, Maoqing Tian, Shuyang Sun, et al. Spindle net: Person re-identification with human body region guided feature decomposition and fusion. In *CVPR*, 2017. 1
- [73] Liang Zheng, Zhi Bie, Yifan Sun, Jingdong Wang, Chi Su, Shengjin Wang, and Qi Tian. Mars: A video benchmark for large-scale person re-identification. In *ECCV*, pages 868–884. Springer, 2016. 5, 6, 11

- [74] Wei-Shi Zheng, Shaogang Gong, and Tao Xiang. Person re-identification by probabilistic relative distance comparison. In *CVPR*, 2011. [8](#)
- [75] Wei-Shi Zheng, Xiang Li, Tao Xiang, Shengcai Liao, Jianhuang Lai, and Shaogang Gong. Partial person re-identification. In *ICCV*, 2015. [2](#)
- [76] Kaiyang Zhou, Yongxin Yang, Andrea Cavallaro, et al. Omni-scale feature learning for person re-identification. *ICCV*, 2019. [2](#), [4](#), [8](#), [9](#)
- [77] Jiaxuan Zhuo, Zeyu Chen, Jianhuang Lai, and Guangcong Wang. Occluded person re-identification. In *ICME*, pages 1–6. IEEE, 2018. [2](#)